# Intermixing and Three-Dimensional Islands in the Epitaxial Growth of Au on Ag(110)

S. Rousset,[a] S. Chiang, D. E. Fowler, and D. D. Chambliss

*IBM Research Division, Almaden Research Center, 650 Harry Road, San Jose, California 95120-6099*

(Received 10 February 1992)

The epitaxial growth of Au on Ag(110) has been studied by scanning tunneling microscopy up to 2.5 ML. In the submonolayer range the results show that gold atoms are intermixed with the silver atoms in the top two layers. Above 1 ML, a two-dimensional fingerlike growth gives rise to anisotropic three-dimensional islands of gold. This "intermixed Stranski-Krastanov" growth mode is in quantitative agreement with ion channeling data which were previously interpreted as a bilayer growth mode [Fenter and Gustafson, Phys. Rev. Lett. **64**, 1142 (1990)].

PACS numbers: 68.35.Bs, 61.16.Di, 61.16.Fk, 68.55.Jk

Predicting the morphology, atomic arrangement, or degree of epitaxy of a thin film grown on a single-crystal substrate has been a continuing challenge. One goal of interface and thin-film science is to understand the growth process in sufficient detail to manipulate the structure and interface of the film, permitting improvement in thin-film devices. Epitaxial growth has a long history which has led to general classification into three growth modes [1]: Volmer-Weber (VW) growth, three-dimensional (3D) island growth; (2) Frank–van der Merwe (FM) growth, layer-by-layer growth, and (3) Stranski-Krastanov (SK) growth, 3D islands on top of one or a few epitaxial layers. For low strain energy in the film, FM growth typically occurs for overlayers with low surface free energy relative to the substrate, whereas VW growth occurs for those with high surface free energy. For high strain energy in the film, SK growth occurs for low overlayer surface free energy. Additional factors, such as alloying and surface atom mobilities, may influence the growth mode and lead to structures not expected from simple energetics. When overlayer and substrate surface energies and lattice parameters are nearly equal, FM growth usually occurs. Thus FM growth is expected for Au on Ag ($\gamma_{Au}=1.6$ J/m$^2$, $\gamma_{Ag}=1.3$ J/m$^2$; $a_{Au}=4.08$ Å, $a_{Ag}=4.09$ Å), and indeed has been reported for Au on Ag(111) [2] and on Ag(100) [3]. On the more open Ag(110) surface, however, this Letter shows how interfacial alloying gives rise instead to a modified SK mode.

A recent medium-energy ion scattering (MEIS) study of Au on Ag(110) by Fenter and Gustafsson (FG) [4,5] was interpreted as evidence for a bilayer growth mode. We have investigated this system by scanning tunneling microscopy (STM) up to 2.5 monolayers (ML) and show unambiguously that bilayer growth does not occur. The STM results and our reinterpretation of the MEIS data suggest that below 1 ML, atomic exchange leaves almost all Au atoms in the second layer under a top layer of Ag. At higher coverage, 3D anisotropic islands of Au, elongated along the [1$\bar{1}$0] directions, are formed on top of the intermixed layers. Thus, the growth mode of this system, deduced by combining the STM and MEIS results, can be described as an "intermixed Stranski-Krastanov" model. In addition, STM images of intermediate coverages give a unique insight into the transition from 2D to 3D growth: correlated growth of 2D fingers at steps is a kinetic pathway to the formation of 3D islands.

The multichamber ultrahigh vacuum STM apparatus has been described in detail elsewhere [6]. The Ag(110) crystal was cleaned by Ar-ion bombardment (500 eV) and flash annealed at 600 °C. After the sample was allowed to cool for at least 1 h to reach room temperature (RT), it was exposed to Au flux evaporated from a W basket. Au flux was measured using a line-of-sight ionization gauge. The gauge was calibrated for Au within 20% by optimizing the sharp $c(2\times2)$ low-energy electron diffraction (LEED) pattern obtained when $0.5\pm0.1$ ML of Au is deposited onto Cu(100) [7]. Most of the evaporations were performed at a constant rate of 0.6 ML/min (1 $ML_{Ag(110)}=8.45\times10^{14}$ atoms/cm$^2$). Experiments were performed with different deposition rates, ranging from 0.4 to 2 ML/min, without any qualitative changes in the results. Following sample preparation, no contamination of the surface with O or C was found by Auger spectroscopy, and the observed LEED pattern is $(1\times1)$ for all coverages. The STM experiments were performed within a few hours after deposition, and no changes occurred overnight. The STM images were acquired in a constant current mode, mainly with negative sample voltage from 30 mV to 2 V and tunneling current from 1 to 2 nA. Positive sample polarity did not show any spectroscopic effects. Each image was recorded in ~5 min. Linear or quadratic background planes have been subtracted from the images, but further image processing, other than one-dimensional differentiation of Fig. 2(a), was deemed unnecessary.

STM images for $\leq 1$ ML of deposited Au (Fig. 1) show no islands and only monatomic steps, 1.45 Å high, with a half-unit-cell lateral shift of the close-packed rows of neighboring terraces in atomically resolved images [Fig. 1(b)]. While the fairly narrow terraces in Fig. 1 are typical of our slightly misoriented crystal (~1°), no islands or bilayer steps are seen even on terraces as wide as 900 Å. The system appears to be in a perfect $1\times1$ epitaxy [Fig. 1(b)], and the STM data do not distinguish between the Au and Ag atoms because of their similar size.


FIG. 1. STM top view images. (a) Clean Ag(110), showing "frizzy" monatomic steps. (b) Atomic resolution image for 0.3 ML Au on Ag(100) showing stable [1$\bar{1}$0] facets and some frizzy steps. Lengths of axes correspond to 6 unit cells. (c) 1.0 ML Au on Ag(110), with 2D finger growth from monatomic steps.

The clean surface [Fig. 1(a)] shows "frizzy" steps as on some other metal surfaces [8], with two consecutive images acquired from the same area presenting different images. Although interpreted as a dynamic effect, the mechanism of such a motion is not yet understood. At the intermediate coverage of 0.3 ML, the step edges present stable [1$\bar{1}$0] facets with some frizzy step edges. For 1 ML of Au, the steps are imaged stably and 2D finger growth has begun [Fig. 1(c)].

The absence of islands and biatomic steps contradicts the model of Au bilayer growth proposed by FG [4,5] for samples prepared at a similar temperature and deposition rate. We believe the STM and the MEIS data are consistent with each other, but that the previous interpretation of the MEIS data is incorrect. The MEIS data show a "blocking dip curve," proving that the deposited Au atoms are shadowed for Au coverages of $\geq 0.06$ ML. One cannot conclude, however, that the shadowing is due to bilayer growth unless surface alloying or intermixing is ruled out. FG [4,5] argued that there was no intermixing because the Ag yield decreased linearly with the increase in Au coverage up to $\sim 1$ ML. However, due to the openness of the (110) surface, two layers of Ag are exposed to the incident He ions in the MEIS experiment, so that a Au atom in the top or second layer contributes in the same way to the decrease of the Ag yield by reason of symmetry. Thus, the MEIS data are certainly consistent with an intermixing model, and the lack of bilayers in the STM data proves that alloying must take place. Although FG had considered an intermixing model, they concluded that the bilayer model was more consistent and involved fewer parameters [5]. In addition, a recent first-principles total-energy calculation suggests that bilayer growth is actually energetically unfavorable, and that intermixing of Au and Ag should be expected [9].

We have quantitatively reinterpreted the MEIS blocking curve (Fig. 2 in Ref. [4]), allowing for the possibility of the Au bilayer growth and/or Au deposition which includes regions of Au monolayer growth on top of the Ag(110) surface and regions of Au incorporation below the top layer of the Ag(110) surface. The fractions of the surface covered by each of these three possible Au/Ag configurations are fitting parameters of the model to the MEIS data. The MEIS blocking curve data were simulated by standard Monte Carlo type scattering calculations [10], where the surface relaxation and surface Debye temperature (149 K) for clean Ag(110), as determined by Kuk and Feldman [11], were used in our modeling. Standard bulk Debye temperatures, 215 K for Ag and 170 K for Au [12], were used. A surface Debye temperature for Au was derived by setting the surface/bulk ratio of the Debye temperature for Au to be the same as for Ag(110). This parametrization differs from that used in FG's analysis, in which bulklike vibrational amplitudes were assumed for the Au surface layer [5]. The results of our modeling give a best fit to the blocking curve data when all of the Au atoms are located below the top Ag layer at the reported Au coverage of 0.22 ML. Since the blocking curves are essentially the same for Au coverages from 0.06 to $\sim 0.8$ ML [5], this conclusion should be valid for this entire coverage range. To check the sensitivity of the model to the Debye temperatures chosen, we repeated the calculation with Debye temperatures reduced by 10%. In that case, the best fit to the 0.22 ML Au blocking curve put $\sim 75\%$ of the Au atoms below the top Ag layer and the rest of the Au on top of regions of pure Ag. Thus, for submonolayer coverage of Au, the combination of STM data and modeling of the MEIS data give a consistent picture, where the deposited Au atoms and the top Ag layer of the substrate form an intermixed bilayer, with monatomic steps. The MEIS modeling indicates that most, if not all, of the gold atoms are incorporated in the second layer.

We have also investigated the growth of Au on Ag(110) for coverages $> 1$ ML. At $\sim 1$ ML some fingers start to grow from the steps, and at 1.8 ML, widely separated ($\sim 1000$ Å apart) 3D islands are clearly observed [Fig. 2(a)]. The length of the islands ranges from 500 to 2400 Å, their width is between 50 and 250 Å, and the length/width ratio is between 5 and 13 depending on the size of the island. Figure 2(b) shows clearly that the islands are elongated along the direction of the [1$\bar{1}$0] close-packed rows. Thus anisotropic diffusion and/or anisotropic sticking probability on the surface must be involved in the growth of these islands.

For coverages of 1.4 ML (Fig. 3), the images reveal

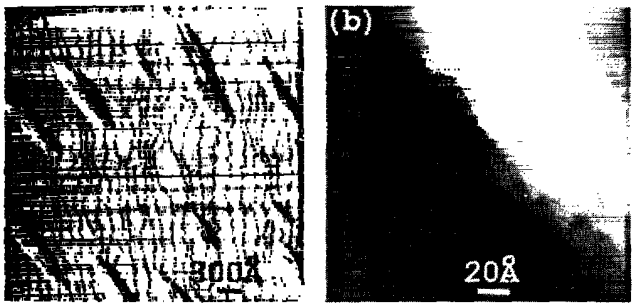


FIG. 2. (a) Differentiated STM image of 1.8 ML Au on Ag(110) shows 3D islands growing across monatomic steps. (b) Atomic resolution image of end of a 3D island shows elongation of island is along close-packed [1$\bar{1}$0] rows.

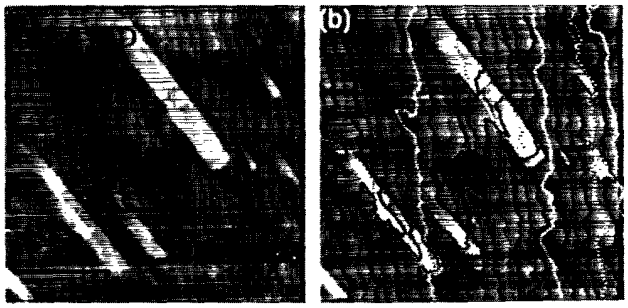


FIG. 3. (a) STM view image for 1.4 ML Au on Ag(110) shows transition in growth from 2D fingers to 3D islands. Labels are explained in text. (b) Same image with lines of constant height drawn along step edges.

the transition in growth modes from 2D fingers to 3D islands. This intermediate regime is characterized by fingers along the [1$\bar{1}$0] direction that grow outward from steps. An isolated finger can grow until it reaches the next downward step, ending in a biatomic step (*A*). Larger structures consist of two or three correlated fingers and can form biatomic or triatomic steps, although there is no particular preference for biatomic steps. More prominent 3D structures are composed of correlated groups of fingers that overlap to form multilayer growth (*B*). The bottom edge (*C*), perpendicular to [1$\bar{1}$0] of these structures, is always a multiatomic step, while the top edge (*D*) is a simple finger grown from the adjacent terrace. While the bottom edges of the fingers are mainly straight, the top ones are more likely divided into two fingers pointing toward the edges of the underlying finger. The straighter end of the bottom step is presumably a lower energy structure, suggesting that the more irregular upper fingers are newer growth. Therefore the growth of a 3D island occurs from the bottom toward the top, with the bottom finger on its terrace growing first, then the next upper one, and so on to the uppermost finger. A finger growing on one step could cause a finger to grow nearby on the next step up, perhaps by its effect on the flux of Au atoms diffusing anisotropically on the surface. Thus, these data show clearly the remarkable result that the growth of 3D originates from the growth of 2D correlated fingers from the steps. Simulations of atomic aggregation in this system are in progress to determine the dynamics of finger correlation leading to 3D growth.

Now we discuss the exact composition of the surface for $\theta > 1$ ML. Since at 1 ML the top layer consists mainly of Ag atoms, Au atoms diffusing on the surface could either intermix with Ag atoms or stay on top to aggregate with other Au atoms. We have investigated these two possibilities quantitatively from calculations based on the MEIS data [4] and also on measurements from the STM data. The surface can be composed of different structures: (1) bare Ag, (2) an intermixed layer which is mainly Ag on top of Au (Ag/Au), (3) Au on top of the intermixed layer (Au/Ag/Au), (4) Au/Au/Ag/Au, and (5) Au/Au/Au/Ag/Au. This model assumes that, after the first layer of Au goes below the Ag surface, the Au grows essentially as pure Ag fingers and islands on top of the surface. The proportions of these structures on the surface determined from this approach are consistent with the MEIS Ag yield and Au $\chi_{\min}$ (Fig. 1 of Ref. [4]) to within the reported experimental errors. Other models, including those having structures with multiple Au layers below a Ag top layer, do not give good quantitative agreement for $\theta \geq 2$ ML. We report only the surface composition determined from the analysis of the MEIS data for $\theta = 1.4$ ML, since, at this coverage, all the layers are easily identified in the STM images. We find excellent agreement between STM and MEIS analyses (Table I), when the 3D structures observed in the STM images are assumed to be composed of only gold. For $\sim 2$ ML Au, the fraction of the surface covered by islands in the STM images also agrees with the MEIS fit.

By combining STM results with reexamination of the MEIS data [4], we have found that Au on Ag(110) at RT grows in an intermixed Stranski-Krastanov mode, starting with a Ag/Au intermixed layer followed by

TABLE I. Percentage of listed layers exposed at surface for Au coverage $\theta = 1.4$ ML on Ag(110), as calculated in fit to MEIS experiment and measured from STM image.

| | Bare Ag | Ag/Au intermix | Au/Ag/Au | Au/Au/Ag/Au | Au/Au/Au/Ag/Au |
|---|---|---|---|---|---|
| MEIS fit | 0 | 64 | 24 | 12 | 0 |
| STM result | 0 | 69 | 24 | 4 | 3 |


FIG. 4. Schematic diagram of "intermixed Stranski-Krastanov" growth mode for Au/Ag(110). Solid (open) circles indicate Au (Ag) atoms. Two circle sizes denote atoms in different vertical (001) planes. Line shows step positions after intermixed layer is complete but before fingers grow. For clarity, steps are drawn more closely spaced than in actual sample.

growth of 3D Au islands (Fig. 4). Since this growth is dramatically different from the deposition of gold on Ag(100) or Ag(111), the open structure of the (110) surface must be responsible for the intermixing process. During the formation of the intermixed layer, Ag-Au exchange must occur, breaking Ag-Ag bonds. Although the details of such exchange are not known for this system, exchange mechanisms for other metal systems have been discussed [13]. After completion of the intermixed layer, further Au growth occurs on top of the Ag surface, despite simple surface free-energy arguments. Surface Ag atoms in the intermixed layer may be too strongly bonded to allow the Au-Ag atom interchange at room temperature necessary for further Au growth below the top Ag layer. Indeed, the sharp reduction of Ag step atom mobility at room temperature when Au is deposited (Fig. 1) suggests such an increase in bond strength. Above 1 ML, Au forms clusters, rather than wetting the surface, presumably because the surface free energy of the intermixed layer is lower than that of Au. The observed 2D correlated fingers which grow from neighboring step edges subsequently overgrow one another and become anisotropic 3D islands.

We would like to acknowledge M. Altman for help in cleaning the Ag(110) crystal, C. T. Chan and K.-M. Ho for sending preprints of Ref. [9], R. Tromp for providing the MEIS Monte Carlo program, and helpful discussions with W. Egelhoff, J. H. Kaufman, and R. J. Wilson. This work was partially supported by the Office of Naval Research (N00014-89-C-0099).

[a]Permanent address: Groupe de Physique des Solide, CNRS–Université de Paris VII, Tour 23, 2 Place Jussieu, 75251 Paris CEDEX 05, France.

[1] E. Bauer, Z. Kristallogr. **110**, 372 (1958); Appl. Surf. Sci. **11/12**, 479 (1982).
[2] R. J. Culbertson, L. C. Feldman, P. J. Silverman, and H. Boehm, Phys. Rev. Lett. **47**, 657 (1981).
[3] T. C. Hsieh, A. P. Shapiro, and T.-C. Chiang, Phys. Rev. B **31**, 2541 (1985).
[4] P. Fenter and T. Gustafsson, Phys. Rev. Lett. **64**, 1142 (1990).
[5] P. Fenter and T. Gustafsson, Phys. Rev. B **43**, 12195 (1991).
[6] S. Chiang, R. J. Wilson, Ch. Gerber, and V. M. Hallmark, J. Vac. Sci. Technol. A **6**, 386 (1988).
[7] G. W. Graham, Surf. Sci. **184**, 137 (1987).
[8] J. Wintterlin, R. Schuster, D. J. Coulman, G. Ertl, and R. J. Behm, J. Vac. Sci. Technol. B **9**, 902 (1991); J. Frohn, M. Giesen, M. Poensgen, J. F. Wolf, and H. Ibach, Phys. Rev. Lett. **67**, 3543 (1991).
[9] K.-P. Bohnen, C. T. Chan, and K. M. Ho, Surf. Sci. Lett. **268**, L284 (1992); C. T. Chan, K.-P. Bohnen, and K. M. Ho, Phys. Rev. Lett. **69**, 1672 (1992).
[10] J. F. Van der Veen, Surf. Sci. Rep. **5**, 199 (1985).
[11] Y. Kuk and L. C. Feldman, Phys. Rev. B **30**, 5811 (1984).
[12] D. S. Gemmel, Rev. Mod. Phys. **46**, 129 (1974).
[13] P. J. Feibelman, Phys. Rev. Lett. **65**, 729 (1990); G. L. Kellogg and P. J. Feibelman, Phys. Rev. Lett. **64**, 3143 (1990).